Dalton Transactions

Accepted Manuscript

ROYAL SOCIETY OF CHEMISTRY

www.rsc.org/dalton

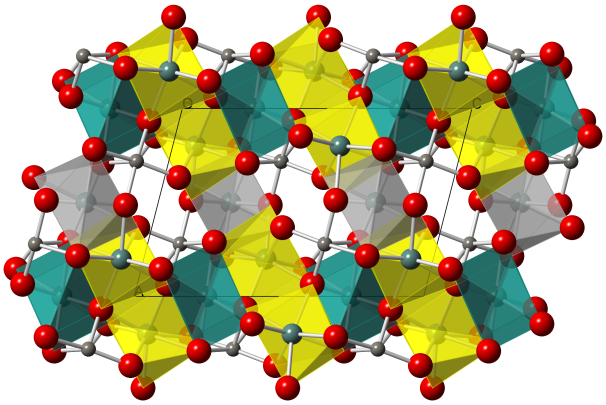

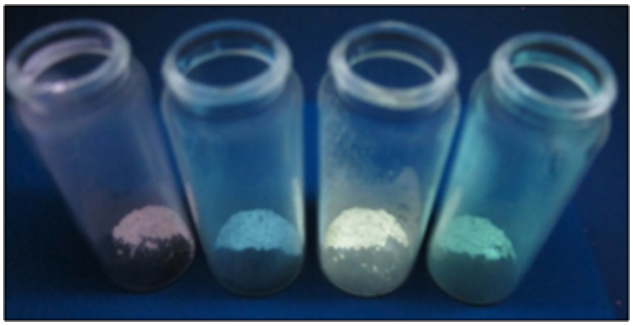

Color-tunable Y_2WO_6 microstructures doped or co-doped with Sm^{3+}, Eu^{3+}, Tb^{3+}, Dy^{3+} were synthesized in the presence of glycerol as solvent and structure directing agent for obtaining white light emitting materials.

Journal Name

ARTICLE

Dopant and excitation wavelength dependent color-tunable white light-emitting Ln^{3+}: Y_2WO_6 materials (Ln^{3+} = Sm, Eu, Tb, Dy)

Rik Van Deun,[a,*] Dorine Ndagsi,[a] Jing Liu,[a,c] Isabel Van Driessche,[d] Kristof Van Hecke,[b] Anna M. Kaczmarek[a,*]

Received 00th January 20xx,
Accepted 00th January 20xx

DOI: 10.1039/x0xx00000x

www.rsc.org/

Microstructured Y_2WO_6 materials were prepared in a hydrothermal synthesis in the presence of glycerol, which was employed as both solvent and structure directing agent, after which it was heat treated at 1100 °C. This material, similar to other previously reported Y_2WO_6 as well as other rare-earth tungstate structures, showed interesting luminescence properties. Six Ln^{3+} doped or co-doped samples, which showed white light emission, are described in this paper. It was observed that the doping ion(s)/doping percentage, heat treatment of the material, as well as the chosen excitation wavelength could be used to tune the emission color of the samples to obtain white light with a warmer or colder undertone. The luminescence lifetimes, quantum yields, CIE coordinates and correlated color temperatures for these samples were determined. Additionally for the co-doped Y_2WO_6 samples the energy transfer mechanisms were proposed as after heat treatment a significant change in the luminescence properties was observed. This can be linked to the conversion from distorted tungstate groups in the precursor material to regular tungstate groups in the heat treated material.

1. Introduction

Rare-earth tungstate materials at the nano- and micro- size have received a considerable amount of attention in the last few years.[1-6] These materials have good thermal and chemical stability, as well as broad near-UV charge transfer bands. When doped with trivalent lanthanide ions, rare-earth tungstate materials have shown to have interesting luminescence properties with potential applications in various fields. These materials can be exited through the broad W-O charge transfer band, which is more efficient then exciting into the narrow f-f transitions of trivalent lanthanides, which are parity-forbidden and therefore have low molar absorption coefficients.[7] One of the promising aspects of the tungstate materials is the possibility to obtain white light emission from a single material.[8-10] Because the rare-earth tungstate matrix itself emits in the blue-green region, in combination with narrow-line emission of doped lanthanide ions it can yield white light.

Up to date many rare-earth tungstate materials with fascinating architectures (ranging from 0D to 3D structures) have been reported in literature. Materials such as $RE_2(WO_4)_3$, RE_2WO_6, $NaRE(WO_4)_2$, $RE(WO_3)_2(OH)_3$ have been obtained in a variety of syntheses with the hydrothermal reaction, microwave assisted hydrothermal reaction, sol-gel processing, and molten salt synthesis being the most commonly employed.[1] Various factors such as the presence of an organic ligand, reaction pH, reaction time and temperature, as well as the source of both lanthanide and tungstate ions influence the phase and morphology of the formed materials.[1] In the past two years a growing interest in the topic of luminescent lanthanide doped rare-earth tungstate materials has yielded a large amount of publications. In a few of them report of high quantum yields of these materials can be found. In our recent publication we reported Ln^{3+} doped Y_2WO_6 (Ln = Sm, Eu, Dy) 3D microstructures obtained in a hydrothermal reaction in the presence of sodium dodecyl sulfate surfactant.[5] Some of these materials showed high quantum yields and several yielded white light emission. We observed that when these materials were additionally co-doped with an appropriate amount of Gd^{3+} ions the luminescence properties could be significantly increased (quantum yields up to 79%). These interesting luminescence results have encouraged us to further study Y_2WO_6 materials obtained in different reaction condition, and therefore yielding new morphologies.

In this research, glycerol was employed as the solvent as well as the ligand, which controlled the size and shape of the

[a] L^3, Luminescent Lanthanide Lab, Department of Inorganic and Physical Chemistry, Ghent University, Krijsglaan 281-S3, B-9000 Ghent, Belgium; corresponding email: anna.kaczmarek@ugent.be, rik.vandeun@ugent.be
[b] XStruct, Department of Inorganic and Physical Chemistry, Ghent University, Krijsglaan 281-S3, B-9000 Ghent, Belgium.
[c] Key Laboratory of Ministry of Education for Advanced Materials in Tropical Island Resources, Hainan University, Haikou 570228, China.
[d] SCRiPTS, Department of Inorganic and Physical Chemistry, Ghent University, Krijsglaan 281-S3, B-9000 Ghent, Belgium.
Electronic Supplementary Information (ESI) available: Additional luminescence graphs and tables. See DOI: 10.1039/x0xx00000x

synthesized material. Organic ligands are known to form complexes with the metal ions and, therefore, to slow down the nucleation and growth of the crystals (which affects their size and shape). Additionally, the functional groups of the ligand bind to the surface of the material, which affects the growth rate of certain crystal facets.[11] To the best of our knowledge, there has been no systematic study of the effect of glycerol on the phase and morphology formation of the Y_2WO_6 material. A pH of 13 was found to be appropriate to obtain pure phased materials.

Despite the growing amount of reported lanthanide doped rare-earth tungstate materials, there is still a lack of more detailed luminescence data (beyond recording emission and excitation spectra and calculating CIE color coordinates) especially for the white light emitting samples. Although several authors have claimed that these materials could be potentially used in white light phosphor converting LEDs, not enough detailed research on the luminescence of these materials has been carried out to truly assess this.

As synthesizing new, more efficient white-light emitting materials is continuously a topic of great interest we have reported our finding in this publication. A recent review on the topic of white light in a single host by Shang et al. is brought to the reader's attention.[12]

2. Experimental

2.1. Synthesis

All chemicals were of analytical grade and used without further purification.

Samples were synthesized hydrothermally in the presence of glycerol. First 20 mL of glycerol were mixed with 10 mL of distilled water. Next, 1 mmol of the $RE(NO_3)_3 \cdot 6H_2O$ salts at the right percentage were dissolved in 10 mL of distilled water and slowly added to the glycerol/water mixture under stirring on a magnetic stirrer. After 15 minutes, 1 mmol of $Na_2WO_4 \cdot 2H_2O$ dissolved in 10 mL distilled water was added. The pH of the solution was adjusted to 13 by addition of ammonia solution. After further stirring the solution for 10 minutes it was transferred into an autoclave, which was sealed and heated at 200 °C for 24 h (at an oven heating rate of 1 °C/min). The autoclave was allowed to cool naturally to room temperature, the precipitate was centrifugated and washed three times with distilled water and three times with ethanol. The product was dried in a vacuum oven at 55 °C overnight. Some of the samples were further heat treated at 900 or 1100 °C for 3 h (they are referred to as HT).

2.2. Characterization

SEM measurements were performed using a FEI Quanta 200 FSEM and an FEI Nova 600 Nanolab Dual-Beam focused ion beam in secondary electron mode. XRD patterns were recorded by a Thermo Scientific ARL X'TRA diffractometer equipped with a Cu Kα (λ = 1.5405 Å) source, a goniometer and a Peltier cooled Si (Li) solid state detector. Chemical bonding was analyzed by infrared spectroscopy, using a Thermo Scientific FTIR spectrometer (type Nicolet 6700) equipped with a DRIFTS-cell. Samples were prepared by mixing the powders with KBr. The samples were measured in the 550-4000 cm^{-1} range. The luminescence of solid samples was studied. Solid powdered samples were put between quartz plates (Starna cuvettes for powdered samples, type 20/C/Q/0.2). Luminescence measurements were done on an Edinburgh Instruments FLSP920 UV-vis-NIR spectrometer setup. A 450W xenon lamp was used as the steady state excitation source. Luminescence decay times were recorded using a 60W pulsed Xe lamp, operating at a frequency of 100 Hz. A Hamamatsu R928P photomultiplier tube was used to detect the emission signals in the near UV to visible range. All of the luminescence measurements were recorded at room temperature. In order to compare the measurements the same amounts of powders were used as well as the same settings for each measurement (same slit size, step, and dwell time). All emission spectra in the manuscript have been corrected for lamp spectrum. The CIE (Commission Internationale de l'Eclairage) color coordinates and correlated color temperatures (CCT) were calculated using ColorCalculator 4.97 freeware program provided by Osram Sylvania. All of the CIE diagrams presented in the manuscript have assigned coordinates for when the sample is excited into the maximum of the W-O band.

The luminescence decay curves of the samples were measured when excited into the maximum of the W-O band and monitored at the appropriate wavelength. The decay curves could be well fitted using a single exponential equation (1):

$$I = I_0 \exp\left(-\frac{t}{\tau}\right) \quad (1)$$

where I and I_0 are the luminescence intensities at time t and 0, respectively, and τ is the luminescence lifetime. Absolute quantum yields of the heat treated samples were determined using an integrating sphere. Quantum yields were calculated using equation (2):

$$\eta = \frac{\int L_{emission}}{\int E_{blank} - \int E_{sample}} \quad (2)$$

where $L_{emission}$ is the integrated area under the emission spectrum, E_{blank} is the integrated area under the "excitation" band of the blank, and E_{sample} is the integrated area under the excitation band of the sample (as the sample absorbs part of the light, this area will be smaller than E_{blank}).

3. Results and discussion

3.1. Structure and morphology

The XRD patterns of the samples before heat treatment could not be matched to a pure Y_2WO_6 crystallographic phase. After the samples were heat treated at 900 °C or 1100 °C, the XRD patterns could be best matched with the XRD pattern of monoclinic Y_2WO_6 calculated using the Mercury crystal structure visualization, exploration, and analysis tool. Figure 1 presents examples of an XRD pattern showing the material before heat treatment, after heat treatment at 900 °C and

after heat treatment at 1100 °C. Additionally the standard XRD pattern of monoclinic Y_2WO_6 has been presented. Heat treatment of the material at 900 °C led to a mixture of the tetragonal and monoclinic Y_2WO_6 phase. Only when the heat treatment temperature was increased to 1100 °C the pure

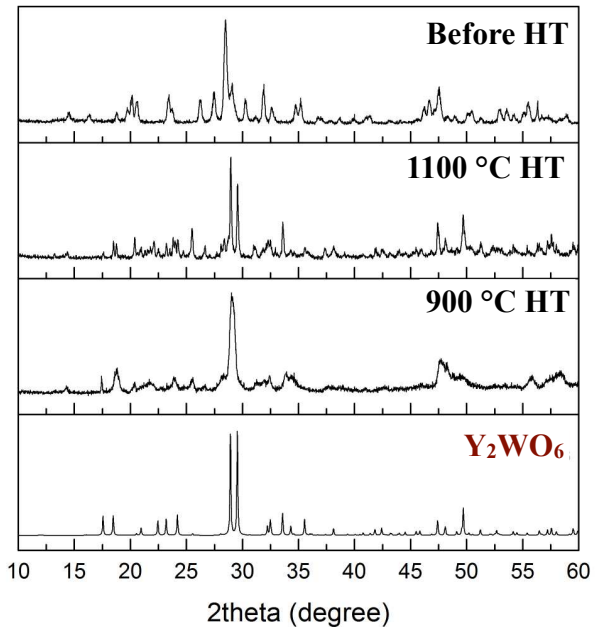

Figure 1. XRD patterns of the material as obtained (before HT), heat treated at 900 °C, and heat treated at 1100 °C. The standard monoclinic Y_2WO_6 XRD pattern has been presented at the bottom.

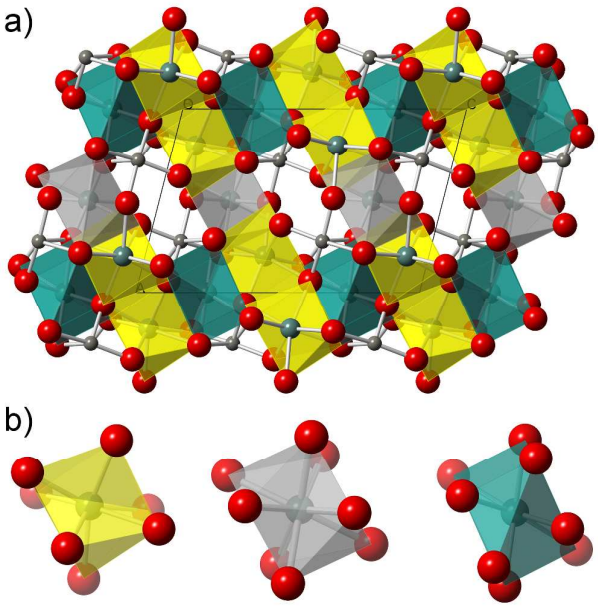

Figure 2. a) Crystal structure of monoclinic Y_2WO_6 in the P2/c space group. Y^{3+} ions are presented in grey, W^{6+} in blue and O^{2-} in red. b) The three different colored polyhedrons represent the three non-equivalent Y^{3+} sites.

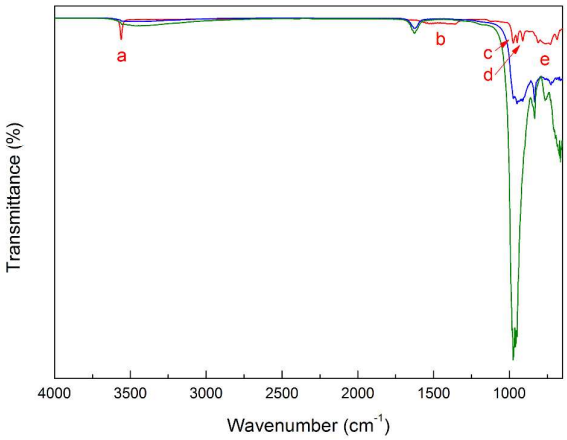

Figure 3. DRIFTS spectra of undoped Y_2WO_6 material before heat treatment (red), after heat treatment at 900 °C (blue), and heat treated at 1000 °C (green).

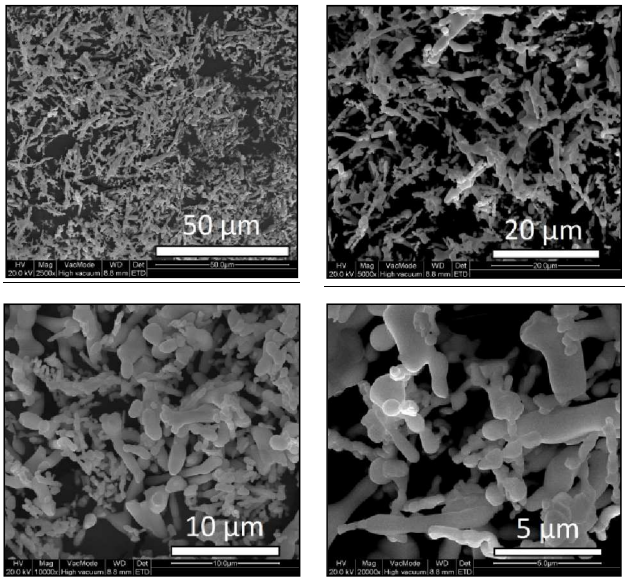

Figure 4. SEM images of the Y_2WO_6 material heat treated at 1100 °C presented at different magnifications.

monoclinic Y_2WO_6 was obtained. It has been reported before that Y_2WO_6 forms a metastable phase.[3] Upon heat treatment at 650 °C, Wang et al. reported obtaining a cubic phase. Heat treating at a higher temperature of 750 °C yielded the tetragonal phase and only raising the temperature to 1000 °C resulted in a pure monoclinic phase. No changes in the XRD patterns were observed after doping the Y_2WO_6 samples with Ln^{3+} ions. Crystal structures of Y_2WO_6 with three different space groups: P2/c, $P2_12_12_1$, and P4/nmm (where Y_2WO_6 with $P2_12_12_1$ space group has two polymorphs with different unit cells) have been reported in literature and can be found in the Inorganic Crystal Structure Database (ICSD).[13-16] The monoclinic Y_2WO_6 has a P2/c space group with a = 7.589 Å, b = 5.334 Å, c = 11.354 Å, β = 104.41 °, and Z = 4. The crystal

structure of the monoclinic Y_2WO_6 has been presented in Figure 2. From the structure it can be seen that there are three nonequivalent Y^{3+} lattice sites. Two of these lattice sites are eight-coordinated by eight O^{2-} ions, and one Y^{3+} lattice site is coordinated by seven O^{2-} ions. All of the W^{6+} ions are surrounded by six oxygen ions and form WO_6 octahedra. The ionic radii of the Ln^{3+} ions (e.g. for Eu^{3+} ionic radius is 1.07 Å) resemble the Y^{3+} ionic radius (1.02 Å) more than the W^{6+} ionic radius (0.60 Å). Therefore, the doped lanthanide ions occupy the Y^{3+} crystallographic sites. The Ln^{3+} ions can substitute the Y^{3+} ions in any of the three crystallographic sites. The two 8 coordinated Y^{3+} ions can be described as cubes distorted in the direction of an antiprism, whereas the 7 coordinated Y^{3+} ion is a distorted cube with one corner missing. The symmetry of the two 8 coordinated Y^{3+} ions is C_2 and the symmetry of the 7 coordinated Y^{3+} ion is C_1. It has been reported before that for the Y^{3+} ions with C_2 symmetry can incorporate doped Eu^{3+} ions in equal amounts. As they are almost identical, we would expect to see only two different Eu^{3+} coordination sites in Eu^{3+} doped Y_2WO_6 material.[17]

To further characterize the materials DRIFTS spectra of an undoped Y_2WO_6 material before and after heat treatment (both at 900 °C and 1100 °C) were recorded and have been presented in Figure 3. The sharp band at 3559 cm^{-1} (band "a") can be assigned to the O-H stretching vibrations of water and/or glycerol. This band is no longer present in the samples, which were heat treated. Band "b" at around 1406 cm^{-1} can also be attributed to the O-H stretch vibrations of water/glycerol. Below 1000 cm^{-1} the characteristic tungstate vibrations are present. Bands "c" and "d" can be assigned to the W-O stretch vibrations and band "e" to the asymmetric stretch vibrations of W-O-W bridges.[18]

Next, the morphology of the undoped Y_2WO_6 sample was characterized by SEM, as shown in Figure 4. The SEM images revealed that irregular micro-sized rod-like structures were formed. Additionally some spherical particles that are smaller in size are also present. Based on these images it can be presumed that initially spherical particles were formed, which had then formed the rod-like structures.

3.2. Luminescence properties

Rare-earth tungstates at the nano- and micro- size have been reported to be good host lattices for the luminescence of lanthanide ions.[1,3,5,9,11] Yttrium compounds are suitable hosts, because they are spectroscopically silent, therefore no f-f transitions are possible, unless other lanthanide ions are incorporated into the materials. The tungstate materials themselves emit blue-green light under ultraviolet excitation.[5] The excited tungstate groups may effectively transfer energy to doped lanthanide ions. In this study we investigated the possibility to obtain white light emission from Y_2WO_6 material doped or co-doped with Sm^{3+}, Eu^{3+}, Dy^{3+}, and Tb^{3+} ions at different concentrations. Six samples, which showed white light emission in the precursor material (before heat treatment) or/and after heat treatment (HT) were chosen for further detailed investigation.

In general in all of the samples a broad charge transfer band is visible in the excitation spectra of both the precursor samples as well as the heat treated samples. Mostly in the precursor Y_2WO_6 materials the maximum of this band is located around 260-270 nm, whereas after heat treatment the band shifts towards longer wavelengths (band maxima located around 300 nm). In the precursor materials some weak sharp peaks, which can be assigned to the transitions of trivalent lanthanides, are observed. These transitions are usually not present in the heat treated materials. In the emission spectra of the precursor materials broad charge transfer bands of different intensities are present besides the characteristic emission peaks of the lanthanides. Their presence indicates that the transfer of energy from the W-O charge transfer band to the Ln^{3+} ions is not complete. The broad W-O band located in the blue color region in combination with emission of the Ln^{3+} ions in some cases yields white light emission. After heat treatment the W-O band is much weaker or not present at all in the samples suggesting a more efficient transfer of energy in the regular tungstate groups compared to the distorted tungstate groups.

3.2.1. Luminescence properties of single Ln^{3+} doped Y_2WO_6

3.2.1.1. 1% Dy^{3+} doped Y_2WO_6

1% Dy^{3+} doping into the Y_2WO_6 matrix yielded white light emitting materials both before and after heat treatment. The excitation and emission spectra of the 1%Dy: Y_2WO_6 and 1%Dy: Y_2WO_6 HT samples are presented in Figure S1 and Figure S2. After heat treatment a shift of the W-O charge transfer band towards longer wavelengths is observed. In the emission spectrum of the 1%Dy: Y_2WO_6 sample a strong broad W-O band is present, which overlaps the characteristic Dy^{3+} transition peaks. This indicates an insufficient transfer of energy from the tungstate band to the Dy^{3+} ions. After heat treatment the sample contains three sharp peaks, which can be assigned to the typical intra-4f transitions of Dy^{3+}. The peak at 479.4 nm can be assigned to the $^4F_{9/2}$ -> $^6H_{15/2}$ transition, the peak at 578.5 nm to the $^4F_{9/2}$ -> $^6H_{13/2}$ transition, and the one at 671.1 nm to the $^4F_{9/2}$ -> $^6H_{11/2}$ transition. Additionally a weak broad band is present in the low wavelength region of the spectrum and partially overlaps with the $^4F_{9/2}$ -> $^6H_{15/2}$ transition. This band can be assigned to the W-O charge transfer band. Figure 5 presents the emission spectrum of 1%Dy: Y_2WO_6 HT sample with a rainbow curve fitted underneath to show the different color components, as well as a CIE color diagram which shows the emitted colors of the 1%Dy: Y_2WO_6 and 1%Dy: Y_2WO_6 HT samples. In the case of the 1%Dy: Y_2WO_6 sample light blue emission is obtained and for the 1%Dy: Y_2WO_6 HT sample white light with a yellow overtone is observed. The white light emitting 1%Dy: Y_2WO_6 HT sample showed a luminescence lifetime of 229 µs and an absolute quantum yield of 11%.

The 1%Dy: Y_2WO_6 HT sample was additionally excited at different wavelengths into the charge transfer band to

investigate the change in the emission spectrum and therefore also emitted color. Figure 6 presents an emission map of the sample excited at wavelengths ranging from 250 nm – 330 nm. At all tested excitation wavelengths white light emission was obtained, but with more or less yellow overtone (see Figure 6 and Table S3).

In both cases (the precursor and heat treated sample) when placed under a UV lamp at excitation wavelengths of 254 nm (see Figure 7) and 365 nm white light emission was observed.

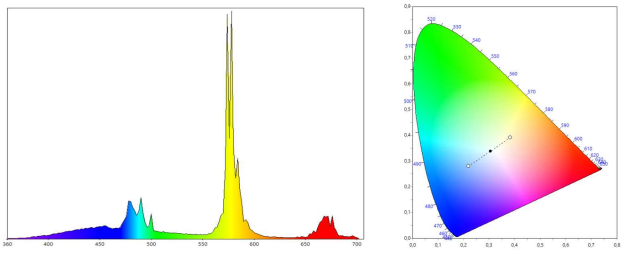

Figure 5. Left: Emission spectrum of 1%Dy: Y_2WO_6 HT with rainbow curve fitted underneath to show the different color components (sample excited at 299.6 nm). Right: CIE color diagram presenting the emitted color of the 1%Dy: Y_2WO_6 (left white point) and 1%Dy: Y_2WO_6 HT (right white point).

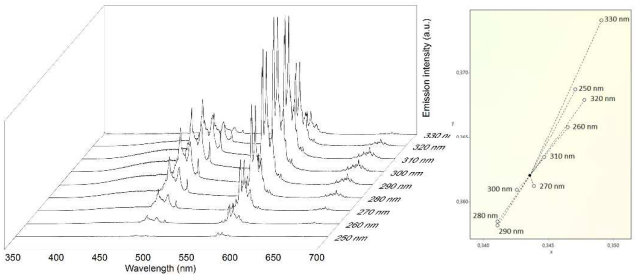

Figure 6. Left: emission map of 1%Dy: Y_2WO_6 HT material excited into the W-O band at different wavelengths. Right: zoom in of the CIE color diagram of 1%Dy: Y_2WO_6 HT material when excited at wavelengths ranging from 250 nm – 330 nm.

Figure 7. Photo of 1%Dy: Y_2WO_6 before heat treatment (a) and after heat treatment (b) when placed under a UV lamp with a 254 nm excitation wavelength.

3.2.1.2. 1% and 3% Sm^{3+} doped Y_2WO_6

1% Sm^{3+} and 3% Sm^{3+} doping into the Y_2WO_6 matrix yielded light blue and white-blue emission, respectively before heat treatment and orange emission in both cases after heat treatment. When these samples were placed under a UV lamp (254 nm and 365 nm excitation wavelengths) white light (with pink or green overtones) was observed. The excitation and emission spectra of the 1% and 3% Sm: Y_2WO_6 and 1% and 3% Sm: Y_2WO_6 HT samples are presented in Figure S3-S6.

As in the case of the 1% Dy^{3+} doped samples after heat treatment a shift of the W-O charge transfer band towards longer wavelengths is observed. Also it can be seen that the W-O band becomes significantly broader in the HT samples. In the emission spectra of the 1% and 3% Sm: Y_2WO_6 samples a strong broad W-O band is present, which overlaps the characteristic Sm^{3+} transition peaks. After heat treatment the characteristic transitions of Sm^{3+}: $^4G_{5/2}$ -> $^6H_{5/2}$, $^4G_{5/2}$ -> $^6H_{7/2}$, $^4G_{5/2}$ -> $^6H_{9/2}$, and $^4G_{5/2}$ -> $^6H_{11/2}$ are present in the spectra, as well as weak W-O charge transfer bands in the lower wavelength region. The significant decrease of the W-O band after heat treatment indicated that the transfer of energy is much more efficient in the materials which had been heat treated. The decay time for the 1%Sm: Y_2WO_6 HT sample was determined to be 662 µs, whereas for the 3%Sm: Y_2WO_6 HT sample it had dropped to 470 µs. Therefore as can be seen in the 3% Sm: Y_2WO_6 HT concentration quenching is observed. The low critical quenching concentration of the Sm^{3+} ions (compared to for example Eu^{3+} ions) may be due to the cross-relaxation effect of these ions.[5]

3.2.1.3. 3% Eu^{3+} doped Y_2WO_6

When the Y_2WO_6 material was doped with 3% Eu^{3+} ions white light emission was obtained for the as obtained sample, and red emission for the sample after heat treatment. Figure 8 presents the excitation and emission spectra of the 3% Eu^{3+} doped Y_2WO_6 sample. In the emission spectrum the $^5D_0$ –> ^7F_J transitions peaks of Eu^{3+} are visible (see Table 3 for peak assignment), additionally a weak W-O charge transfer band is present. The charge-transfer band adds a blue light component to the material and therefore in combination with the red light from the Eu^{3+} ions it yields white light emission. After heat treatment the W-O band is no longer present in the emission spectrum (Figure S7) and red emission is obtained. A CIE color diagram (also Figure 8) displays the change of color after heat treatment.

Based on a detailed investigation of the Eu^{3+} relative peak intensities and splitting in the precursor and heat treated sample it can be concluded that the large intensities of the $^5D_0$ –> $^7F_2$ peaks indicates low symmetry. In the precursor sample the $^5D_0$ –> $^7F_0$ peak is not split, also the $^5D_0$ -> $^7F_1$ peak is split two times (suggesting an axial symmetry), therefore most likely only one europium coordinate site exists (or two with very similar symmetry, which would give very much alike transition peak splittings). In the heat treated sample although the $^5D_0$ –> $^7F_0$ peak is not split a larger amount of splittings (four) of the $^5D_0$ –> $^7F_1$ peak indicates more than one europium coordination site in the material.[19] Also a large amount of splitting of the $^5D_0$ –> $^7F_2$ transition peak suggests more than one coordination site. As there are three Y^{3+} sites, which can be substituted with Eu^{3+} ions one would expect up to three different Eu^{3+} coordination site. Yet, as mentioned previously, the two 8 coordination Y^{3+} ions are almost identical, therefore

we expect to see only two different Eu^{3+} coordination sites in Eu doped Y_2WO_6 material.[17]

The decay time for the 3% Eu: Y_2WO_6 sample was determined to be 296 µs. For the 3% Eu: Y_2WO_6 HT sample it had increased to 732 µs. Both the 3% Eu: Y_2WO_6 and 3%Eu: Y_2WO_6 HT sample showed white light emission when placed under a UV lamp (254 nm excitation).

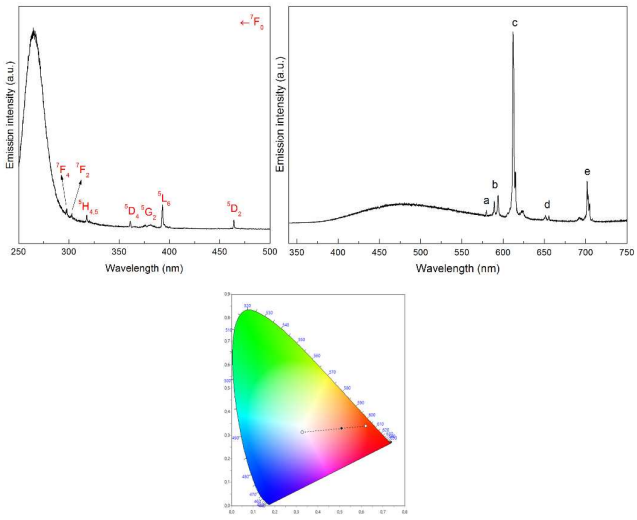

Figure 8. Top left: excitation spectrum of 3% Eu: Y_2WO_6 material (monitored at 612.2 nm). Top right: emission spectrum of 3% Eu: Y_2WO_6 material (excited at 265.7 nm). Bottom: CIE color diagram presenting the emitted color of the 3% Eu: Y_2WO_6 (left white point) and 3% Eu: Y_2WO_6 HT (right white point).

Table 3. Assignment of transitions presented in Figure 8.

Symbol	Wavelength (nm)	Wavenumber (cm^{-1})	Transitions
a	579.4	17259	$^5D_0$ -> $^7F_0$
b	593.4	16852	$^5D_0$ -> $^7F_1$
c	612.2	16335	$^5D_0$ -> $^7F_2$
d	651.0	15361	$^5D_0$ -> $^7F_3$
e	701.8	14249	$^5D_0$ -> $^7F_4$

3.2.2. Luminescence properties of Y_2WO_6 co-doped with two different Ln^{3+} ions

3.2.2.1. 2.5% Eu^{3+}, 2.5% Tb^{3+} co-doped Y_2WO_6

It was observed that when the Y_2WO_6 material was co-doped with appropriate amounts of Eu^{3+} and Tb^{3+} ions white light emission was obtained. The co-doping of Eu^{3+} and Tb^{3+} ions into a material to obtain white light has already been reported in previous publications and depending on the material different ratios of the ions are needed.[6,20] For the Y_2WO_6 material samples co-doped with 2.5% Eu^{3+} and 2.5% Tb^{3+} before heat treatment showed white light emission. After the sample was heat treated the emission color changed to

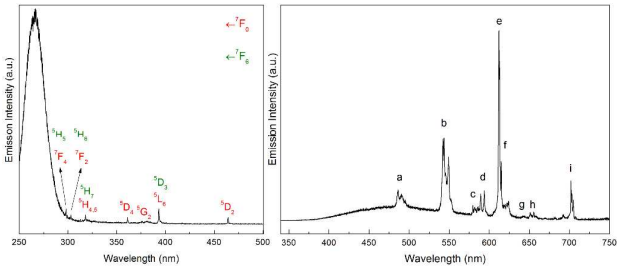

Figure 9. Left: excitation spectrum of 2.5% Eu, 2.5% Tb: Y_2WO_6 material (monitored at 612.2 nm). Right: emission spectrum of 2.5% Eu, 2.5% Tb: Y_2WO_6 material (excited at 267.9 nm).

Table 4. Assignment of transitions presented in Figure 9.

Symbol	Wavelength (nm)	Wavenumber (cm^{-1})	Eu^{3+} transitions	Tb^{3+} transitions
a	486.4	20559		$^5D_4$ -> $^7F_6$
b	542.9	18420		$^5D_4$ -> $^7F_5$
c	579.4	17259	$^5D_0$ -> $^7F_0$	$^5D_4$ -> $^7F_4$
d	593.7	16844	$^5D_0$ - > $^7F_1$	
e	612.0	16340	$^5D_0$ -> $^7F_2$	
f	615.0	16260		$^5D_4$ -> $^7F_3$
g	643.2	15547		$^5D_4$ -> $^7F_2$
h	651.4	15352	$^5D_0$ -> $^7F_3$	$^5D_4$ -> $^7F_1$
i	702.4	14237	$^5D_0$ -> $^7F_4$	

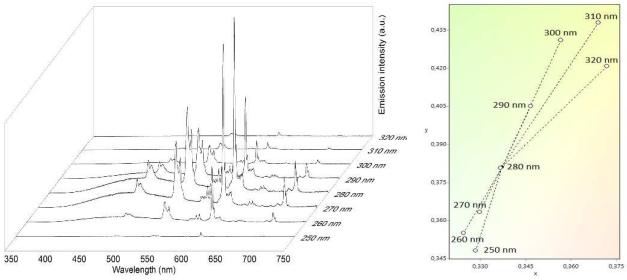

Figure 10. Left: emission map of 2.5% Eu, 2.5% Tb: Y_2WO_6 material excited into the W-O band at different wavelengths. Right: zoom in of the CIE color diagram of 2.5% Eu, 2.5% Tb: Y_2WO_6 material when excited at wavelengths ranging from 250 nm – 330 nm.

orange. Figure 9 presents the excitation and emission spectrum of 2.5% Eu, 2.5% Tb: Y_2WO_6 material. As can be seen both in the excitation and emission spectra transition peaks of Eu^{3+} and Tb^{3+} ions are visible. A broad charge transfer band is present in the 400 – 550 nm region in the emission spectrum and it adds a blue-green color component to the material. All of the emission peaks in Figure 9 have been assigned to the appropriate transition in Table 4. The Eu^{3+} transition peaks are more dominant in the spectrum.

The 2.5 %Eu, 2.5% Tb: Y_2WO_6 sample was excited at different wavelengths into the charge transfer band to investigate the change in the emission spectrum and therefore also emitted

color. Figure 10 presents an emission map of the sample excited at wavelengths ranging from 250 nm – 330 nm. At all the tested excitation wavelengths white light emission was obtained, but with more or less yellow overtone (see Figure 11 and Table S8).

The excitation and emission spectra of the 2.5% Eu, 2.5% Tb: Y_2WO_6 HT materials are presented in Figure S9. Figure 11 presents a photo of the precursor and heat treated 2.5% Eu, 2.5% Tb: Y_2WO_6 samples when placed under a UV lamp at 254 nm excitation.

A proposed energy transfer mechanism for the 2.5% Eu, 2.5% Tb: Y_2WO_6 sample is shown in Figure 12. Upon UV excitation, electrons in the ground state ($^1A_1$) are excited into the ^1B ($^1T_2$) level of the tungstate group, where the electrons relax to their lowest excited ^1B ($^1T_2$) level of the tungstate group, producing emission by the transition to the $^1A_1$ level. Energy can also be transferred from the tungstate group to the Eu^{3+} and Tb^{3+} ions. The excited electrons can relax to the ground states yielding the characteristic emission of both Eu^{3+} and Tb^{3+}. Energy can also be transferred from the $^5D_3$ level of Tb^{3+} to the $^5D_1$ and/or $^5D_0$ levels of Eu^{3+}.

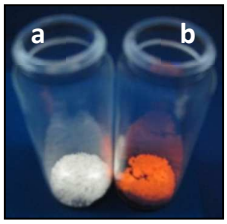

Figure 11. Photo of 2.5% Eu, 2.5% Tb: Y_2WO_6 before heat treatment (a) and after heat treatment (b) when placed under a UV lamp with a 254 nm excitation wavelength.

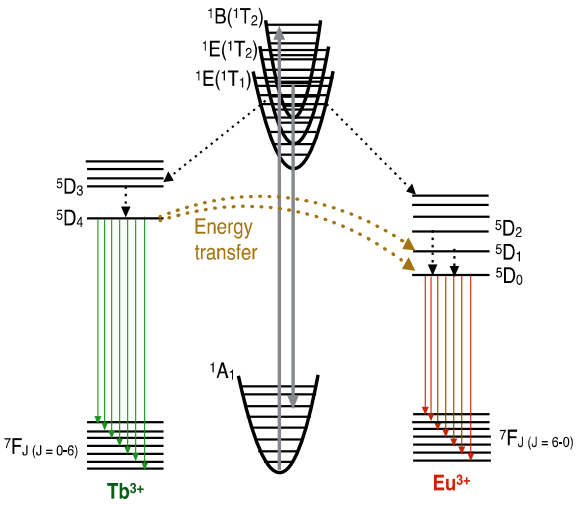

Figure 12. Schematic diagram for the energy transfer from tungstate groups to Eu^{3+} and Tb^{3+} ions, as well as energy transfer from Tb^{3+} to Eu^{3+}.

In the 2.5% Eu, 2.5% Tb: Y_2WO_6 sample after heat treatment the transfer of energy from W-O to Ln^{3+} is more efficient as no charge transfer band is present in the emission spectrum. Also the transition peaks of Tb^{3+} are almost no longer visible in the emission spectrum. As it can be assumed that energy is transferred from the W-O to Tb^{3+} and then passed on to Eu^{3+}, this means that in the heat treated material this process is more efficient than before heat treatment. This can be linked to the conversion from distorted tungstate groups in the precursor material to regular tungstate groups in the heat treated Y_2WO_6 material.

3.2.2.2. 2.5% Sm^{3+}, 2.5% Tb^{3+} co-doped Y_2WO_6

When the Y_2WO_6 material was co-doped with equal amounts of Sm^{3+} and Tb^{3+} ions (2.5%) white light emission (with a shade of green) could be obtained when excited into the charge transfer band. After heat treatment the color changed to orange-red, and when placed under a UV lamp at either 254 nm or 365 nm excitation no white light emission was observed. The excitation and emission spectra of 2.5% Sm^{3+}, 2.5% Tb^{3+}: Y_2WO_6 precursor sample have been presented in Figure 13. When excited at 265.5 nm (into the maximum of the W-O charge transfer band) emission peaks of both Sm^{3+} and Tb^{3+} are observed, although the Tb^{3+} transition peaks are dominant in the spectrum. Besides the narrow emission peaks, which can be assigned to the Ln^{3+} ions, a broad W-O band between 400 – 620 nm is visible. All of the peaks labeled in Figure 13 have been assigned to the appropriate transitions in Table 5.

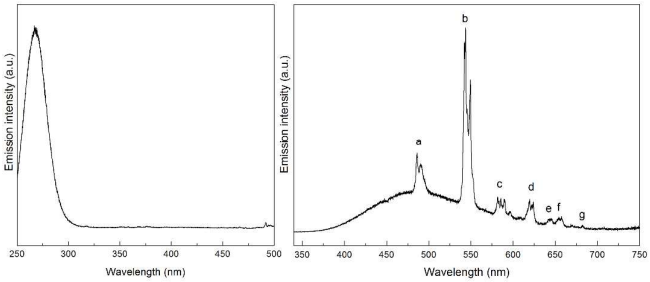

Figure 13. Left: excitation spectrum of 2.5%Sm, 2.5%Tb: Y_2WO_6 material (monitored at 542.0 nm). Right: emission spectrum of 2.5%Sm, 2.5%Tb: Y_2WO_6 material (excited at 265.5 nm).

Table 5. Assignment of transitions presented in Figure 13.

Symbol	Wavelength (nm)	Wavenumber (cm^{-1})	Sm^{3+} Transitions	Tb^{3+} Transitions
a	485.6	20593		$^5D_4$ -> $^7F_6$
b	543.4	18403		$^5D_4$ -> $^7F_5$
c	585.0	17094	$^4G_{5/2}$ -> $^6H_{5/2}$	$^5D_4$ -> $^7F_4$
d	619.2	16150	$^4G_{5/2}$ -> $^6H_{7/2}$	$^5D_4$ -> $^7F_3$
e	643.4	15542	$^4G_{5/2}$ -> $^6H_{9/2}$	$^5D_4$ -> $^7F_2$
f	655.6	15253		$^5D_4$ -> $^7F_1$
g	682.0	14663	$^4G_{5/2}$ -> $^6H_{11/2}$	

In Figure 14 the emission spectrum of 2.5% Sm, 2.5% Tb: Y_2WO_6 HT sample has been presented (excitation spectrum presented in Figure S10). In Figure 15 the emission spectrum

for 2.5% Sm, 2.5% Tb: Y_2WO_6 is presented with a rainbow curve fitted underneath to show the different color components. Additionally a CIE color diagram showing the change in emission color for the precursor and heat treated samples is also shown.

Based on the emission spectra of the precursor and heat treated samples it can be concluded that the energy transfer is more efficient in the material after heat treatment as no W-O band is present. Also only the characteristic emission peaks of Sm^{3+} ions are visible. The Tb^{3+} ions, which were more intensive in the emission spectrum of the precursor sample are no longer visible after heat treatment. A proposed energy transfer mechanism is presented in Figure 16. It can be assumed that in both the precursor and heat treated samples energy is transferred from the tungstate group to both Tb^{3+} and Sm^{3+} ions. Therefore in the emission spectrum of the precursor material characteristic peaks of both lanthanides can be detected. In the heat treated sample energy is most likely transferred from the tungstate group to both Tb^{3+} and Sm^{3+} ions, yet the energy from the Tb^{3+} ions is then transferred to Sm^{3+} which further relax and show the characteristic Sm^{3+} emission peaks.

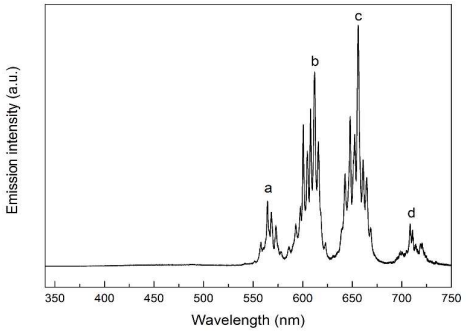

Figure 14. Emission spectrum of 2.5%Sm, 2.5%Tb: Y_2WO_6 HT material (sample excited at 293.7 nm). Labeled peaks have been assigned to the appropriate transitions in Table S10.

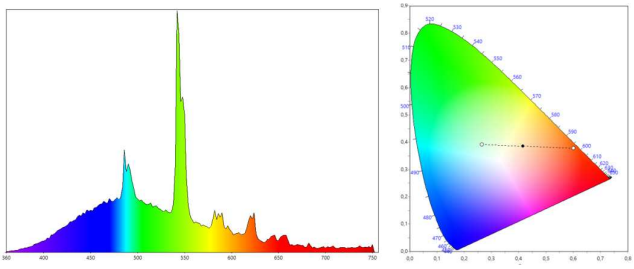

Figure 15. Left: Emission spectrum of 2.5%Sm, 2.5%Tb: Y_2WO_6 with rainbow curve fitted underneath to show the different color components (sample excited at 265.5 nm). Right: CIE color diagram presenting the emitted color of the 2.5%Sm, 2.5%Tb: Y_2WO_6 (left white point) and 2.5%Sm, 2.5%Tb: Y_2WO_6 HT (right white point).

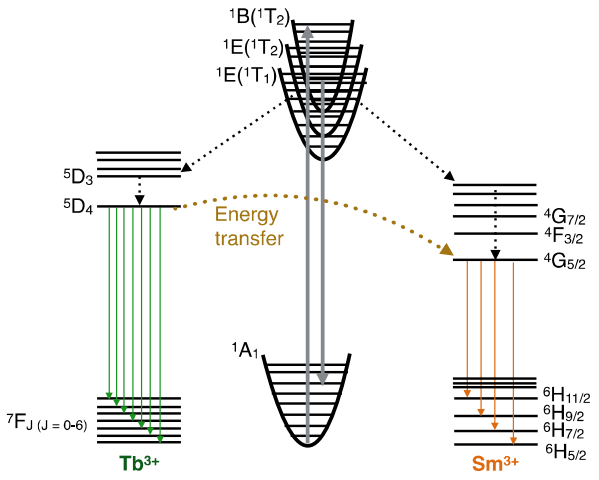

Figure 16. Schematic diagram for the energy transfer from tungstate groups to Tb^{3+} and Sm^{3+} ions, as well as energy transfer from Tb^{3+} to Sm^{3+}.

Table 6. Overview of the CIE coordinates, CCT, and corresponding colors when excited into the maximum of the W-O charge transfer band, as well as when excited with a UV lamp at two chosen wavelengths (254 nm and 365 nm).

Sample	Excited at maximum of W-O charge transfer band				Observed color under UV lamp	
	CIE x	CIE y	CCT (K)	Color	365 nm	254 nm
1%Dy^{3+}: Y_2WO_6	0.219	0.280	26417	Light blue	White	White
1%Dy^{3+}: Y_2WO_6 HT	0.383	0.391	4042	White-yellow	White	White
1%Sm^{3+}: Y_2WO_6	0.228	0.298	17114	Light blue	White	White
1%Sm^{3+}: Y_2WO_6 HT	0.518	0.330	1562	Orange	White-pink	White-pink
3%Sm^{3+}: Y_2WO_6	0.236	0.307	14220	White-blue	Brown	White-green
3%Sm^{3+}: Y_2WO_6 HT	0.551	0.359	1520	Orange-red	Pink	White-green
3%Eu^{3+}: Y_2WO_6	0.327	0.312	5771	White	Brown	White
3%Eu^{3+}: Y_2WO_6 HT	0.621	0.340	1101	Red	Light pink	White
2.5%Eu^{3+}, 2.5%Tb^{3+}: Y_2WO_6	0.347	0.381	5019	White-yellow	White	White
2.5%Eu^{3+}, 2.5%Tb^{3+}: Y_2WO_6 HT	0.630	0.351	1110	Red	Red	Orange
2.5%Sm^{3+}, 2.5%Tb^{3+}: Y_2WO_6	0.266	0.392	8061	White-green	Orange	White-green
2.5%Sm^{3+}, 2.5%Tb^{3+}: Y_2WO_6 HT	0.602	0.378	1347	Orange-red	Light orange	Orange

As it was observed that by varying the excitation wavelength different emission colors were obtained for the samples, therefore Table 6 overviews the investigated samples and presents the emitted color when placed under a laboratory lamp at two excitation wavelengths – 254 nm and 365 nm, as well as the calculated CIE color coordinates and corresponding colors when excited into the maximum of the W-O charge transfer band, as well as the correlated color temperatures. Table 7 overviews the decay times and quantum yields determined for the discussed samples.

Table 7. Luminescence decay times values and absolute quantum yields of the investigated sample before and after heat treatment.

Sample	Decay time [μs]	Quantum yield [%]*
1%Dy^{3+}	16	-
1%Dy^{3+} HT	229	11
1%Sm^{3+}	22	-
1%Sm^{3+} HT	662	16
3%Sm^{3+}	21	-
3%Sm^{3+} HT	470	13
3%Eu^{3+}	296	-
3%Eu^{3+} HT	732	24
2.5%Eu^{3+}, 2.5%Tb^{3+}	418 (Eu^{3+},$^5D_0$ -> $^7F_2$) 597 (Tb^{3+},$^5D_4$ -> $^7F_5$)	-
2.5%Eu^{3+}, 2.5%Tb^{3+} HT	677 (Eu^{3+},$^5D_0$ -> $^7F_2$)	38
2.5%Sm^{3+}, 2.5%Tb^{3+}	507 (Tb^{3+},$^5D_4$ -> $^7F_5$) 475 (Sm^{3+},$^4G_{5/2}$ -> $^6H_{9/2}$)	-
2.5%Sm^{3+}, 2.5%Tb^{3+} HT	461 (Sm^{3+},$^4G_{5/2}$ -> $^6H_{9/2}$)	18

* Due to equipment limitations the absolute quantum yields can only be measured for excitation wavelengths higher than 300 nm

4. Conclusions

In summary, micro-sized Y_2WO_6 materials have been synthesized in a hydrothermal reaction in the presence of glycerol. The luminescence properties of six different Ln^{3+} doped or co-doped samples, which show white light emission either for the precursor material or for the material after heat treatment at 1100 °C were described. It was observed that the color of the Y_2WO_6 microstructures could be tuned not only by the right choice of the doping ion(s) and concentration, heat treatment, but also by varying the excitation wavelength. In the two co-doped systems: 2.5% Eu, 2.5% Tb: Y_2WO_6 and 2.5% Sm, 2.5% Tb: Y_2WO_6 it was observed that the energy transfer mechanisms change after heat treatment. In the precursor samples energy was transferred from the tungstate group to the Eu^{3+} and Tb^{3+} or Sm^{3+} and Tb^{3+} ions. After heat treatment it could be seen that additionally energy transfer from the Tb^{3+} ions to the Eu^{3+} or Sm^{3+} takes place as in the emission spectra no peaks of Tb^{3+} were detectable, and only those of Eu^{3+}/Sm^{3+}.

Acknowledgements

RVD and IVD thank the Hercules Foundation (project AUGE/09/024 “Advanced Luminescence Setup”). KVH and RVD thank the Hercules Foundation (project AUGE/11/029 "3D-SPACE: 3D Structural Platform Aiming for Chemical Excellence"). KVH acknowledges the Research Fund – Flanders (FWO) for funding. IVD thanks Ghent University (project BOFGOA2015000302) for funding.

References

1 A. M. Kaczmarek, R. Van Deun, *Chem. Soc. Rev.,* **2013**, 42, 8835.
2 Z. Hou, Z. Cheng, G. Li, W. Wang, C. Peng, C. Li, P. Ma, D. Yang, X. Kang, J. Lin, *Nanoscale*, 2011, **3**, 1568.
3 J. Wang, Z.-J. Zhang, J.-T. Zhao, H.-H. Chen, X.-X. Yang, Y. Tao, Y. Huang, *J. Mater. Chem.*, 2010, **20**, 10894.
4 Y. Zheng, H. You, K. Liu, Y, Song, G. Jia, Y. Huang, M. Yang, L. Zhang, G. Ning, *CrystEngComm*, 2011, **13**, 3001.
5 A. M. Kaczmarek, K. Van Hecke, R. Van Deun, *Inorg. Chem.,* **2014**, **53**, 9498.
6 Y. Zheng, Z. Li, L. Wang, Y. Xiong, *CrystEngComm*, 2012, **14,** 7043.
7 J. C. G. Bünzli, C. Piguet, *Chem, Soc. Rev.*, 2005, **34**, 1048.
8 A. M. Kaczmarek, Y.-Y. Liu, P. Van Der Voort, R. Van Deun, *Dalton Trans.*, 2013, **42**, 5471.
9 S. Huang, X. Zhang, L. Wang, L. Bai, J. Xu, C. Li, P. Yang, *Dalton Trans*., 2012, **41**, 5634.
10 A. K. Ambast, A. K. Kunti, S. Som, S. K. Sharma, *Appl. Opt*., 2013, **52**, 8224.
11 K. De Keukeleere, J. De Roo, P. Lommens, J. C. Martins, P. Van Der Voort, I. Van Driessche, *Inorg. Chem*. 2015, **54**, 3469.
12 M. Shang, C. Li, J. Lin, *Chem. Soc. Rev.,* 2014, 43, 1372.
13 V. K. Yanovskii, V. I. Voronkova, *Kristallografiya*, 1984, **29**, 904.
14 O. Beaury, M. Faucher, G. T. De Sagey, *Acta* Crystallogr. B, 1981, **37**, 1166.
15 A. V. Tyulin, V. A. Efremov, V. K. Trunov, *Kristallografiya*, 1989, **34**, 885.
16 H. Jinping, X. Jun, L. Hengxin, L. Hongshan, Y. Xibin, L. Yinkang, *J. Solid State Chem*., 2011, **184**, 843.
17 J. A. W. Does de Bye, J. Hornstra, B. Bolger, T. J. A. Pompa, R. A. M. van Ham, *J. Lumin.,* 1989, **43**, 339.
18 F. Lei, B. Yan, *J. Mater. Res*., 2011, **26**, 88.
19 K. Binnemans, *Coord. Chem. Rev*., 2015, doi:10.1016/j.ccr.2015.02.015
20 S.-L. Zhong, L.-F. Zhang, J.-W. Jiang, Y.-H. Lv, R. Xu, A.-W. Xu, S.-P. Wang, *CrystEngComm*, 2011, **13,** 4151.